Research Article

Mingyang Du, Caifang Wu*, He Zhou, Shasha Zhang, and Erchao Zhang

Geochemical characteristics of produced water from coalbed methane wells and its influence on productivity in Laochang Coalfield, China

https://doi.org/10.1515/geo-2020-0124
received April 21, 2020; accepted August 11, 2020

Abstract: The water produced from the coalbed methane (CBM) wells contains abundant geochemical information, which is of great significance in evaluating the productivity of these wells. Based on the data of water produced from five CBM wells, geochemical characteristics of the produced water and its influence on the productivity of the wells are analyzed in Laochang Block. The results show that with the increase in the produced water of the five wells, δD and $\delta^{18}O$ show a downward trend in general, reflecting that the influence of coal seams and surrounding rock on the produced water is weak, while the water–rock interaction of the Y-3 and Y-5 wells is more stable than that of the Y-1, Y-2, and Y-4 wells. Combining the water production characteristics of the Y-3 and Y-5 wells with better drainage and recovery effects, it is proposed that $0 \le \sigma_M < 0.3$ and $0 \le \sigma_Y < 600$ or $0.7 < \sigma_M < 0.8$ and $1{,}200 < \sigma_Y < 1{,}300$, and the fluctuation ranges of Ca^{2+}, Mg^{2+}, HCO_3^- and SO_4^{2-} can provide a basis for quantitative characterization and evaluation of CBM well production.

Keywords: coalbed methane, produced water, geochemical characteristics, coalbed methane well productivity, Eastern Yunnan

* **Corresponding author: Caifang Wu,** Key Laboratory of Coalbed Methane Resource and Reservoir Formation Process, Ministry of Education, Xuzhou, Jiangsu Province, 221008, China; School of Mineral Resources and Geosciences, China University of Mining and Technology, Xuzhou, Jiangsu Province, 221008, China, e-mail: caifangwu@126.com
Mingyang Du, He Zhou, Shasha Zhang, Erchao Zhang: Key Laboratory of Coalbed Methane Resource and Reservoir Formation Process, Ministry of Education, Xuzhou, Jiangsu Province, 221008, China; School of Mineral Resources and Geosciences, China University of Mining and Technology, Xuzhou, Jiangsu Province, 221008, China

1 Introduction

Coal rank, tectonic settings, hydrogeological conditions, and other factors affect the generation and migration of coalbed methane (CBM), among which the hydrogeological conditions are one of the most important [1–3]. Hydraulic dissipation, plugging, and sealing directly affect the occurrence of CBM. At the same time, hydrological conditions control reservoir fluid pressure and water-rich property, which have a great impact on the drainage and reduction of pressure of CBM wells [4–8]. For the desorption and the production of CBM, a large amount of water needs to be discharged [9]. Based on the mechanism of gas migration, researchers have found that the study of the hydrogeochemical characteristics of coal reservoirs can improve the evaluation of the CBM exploration prospects through geological evaluation, gas transport modeling, and physical simulation methods [10–16].

In the CBM wells, during the processes of drainage and methane production, various physical and chemical reactions occur between the water in reservoirs and the surrounding rocks and coal seams. With the prolongation of drainage time, the geochemical characteristics of produced water also change, and the water quality varies with the wells and basins [7,17–19]. The change in the water quality of the produced water with drainage time is the result of mineral dissolution in aquifer [20]. In addition, chemicals injected to improve permeability during coal seam hydraulic fracturing also affect the quality of the produced water in the early stage [21,22]. Existing research shows that the quality of the water produced in CBM wells is poor because of high concentration of sodium ions and the presence of trace elements such as lead and arsenic [10,23].

The amount of water discharged from a well varies considerably at different time intervals as well as for different wells during the same time interval. Furthermore, the amount of hydrogen and oxygen isotopes and trace elements exhibit the same behavior. Therefore, by comparing the water

Open Access. © 2020 Mingyang Du *et al.*, published by De Gruyter. This work is licensed under the Creative Commons Attribution 4.0 International License.

produced from different CBM drainage wells, we can better understand the changes in the water quality [14,24]. In the initial stage, because of the influence of the fracturing fluid, the type of water quality is Na–Cl; in the transitional stage, the type of water quality gradually becomes Na–Cl–HCO_3 because of the constant discharge of the fracturing fluid; in the stable production stage, the type of water quality is Na–HCO_3. From the initial stage to the stable production stage, the concentrations of Na^+, K^+, Cl^-, Ca^{2+}, and Mg^{2+} decrease continuously, HCO_3^- increases gradually, SO_4^{2-} changes slightly, and the salinity decreases significantly until the ion content and geochemical characteristics tend to be stable and close to the original formation water [25,26]. Previous studies on the changes in hydrogen and oxygen isotopes [7,26–28], trace elements [29], and conventional ions [6,30–32] in the produced water have been conducted to varying degrees, but there are few reports on the geochemical characteristics of the produced water from CBM wells in Eastern Yunnan. Based on the latest results of conventional ion, trace element, and hydrogen and oxygen isotope tests of water samples produced by CBM wells in the Laochang Block of Eastern Yunnan, an analysis of the hydrogeochemical characteristics of CBM wells and the influence of surrounding rocks and coal seams on water production was conducted, as well as an evaluation of the influence of the geochemical characteristics of produced water on the performance of the well was conducted. Suggestions are provided for the optimization of the drainage and the production system of the CBM well.

2 Geological background and samples

2.1 Geological background

Laochang Block is located in Fuyuan County, Qujing City, on the southwestern margin of the Yangtze Platform and the inner Laochang anticline zone of the Huangnihe Reflection Arc on the Eastern wing of the second arc of the Shanzi structure in Yunnan Province. The faults in the block are mainly NE-trending, with NW-trending transverse faults and NW-trending arc faults, mainly distributed in the margin of the block. Most of the faults with a drop greater than 100 m are boundary faults, while the internal faults are scarce and mostly distributed near the folds (Figure 1). The main coal-bearing strata are the Upper Permian Longtan Formation with a thickness of 415–475 m. The main coal seams are No. 3, 7 + 8, 16, 17 + 18, and 23. The coal grade is anthracite, black to steel gray, with a glass-like metallic luster, heterogeneous fracture, hardness, and slight brittleness. Coal petrographic composition is mainly semi-dark to semi-bright coal. This area is located in the watershed of the Huangni River, Xijiuxi River, and Seyi River, with high terrain and an undeveloped surface water system.

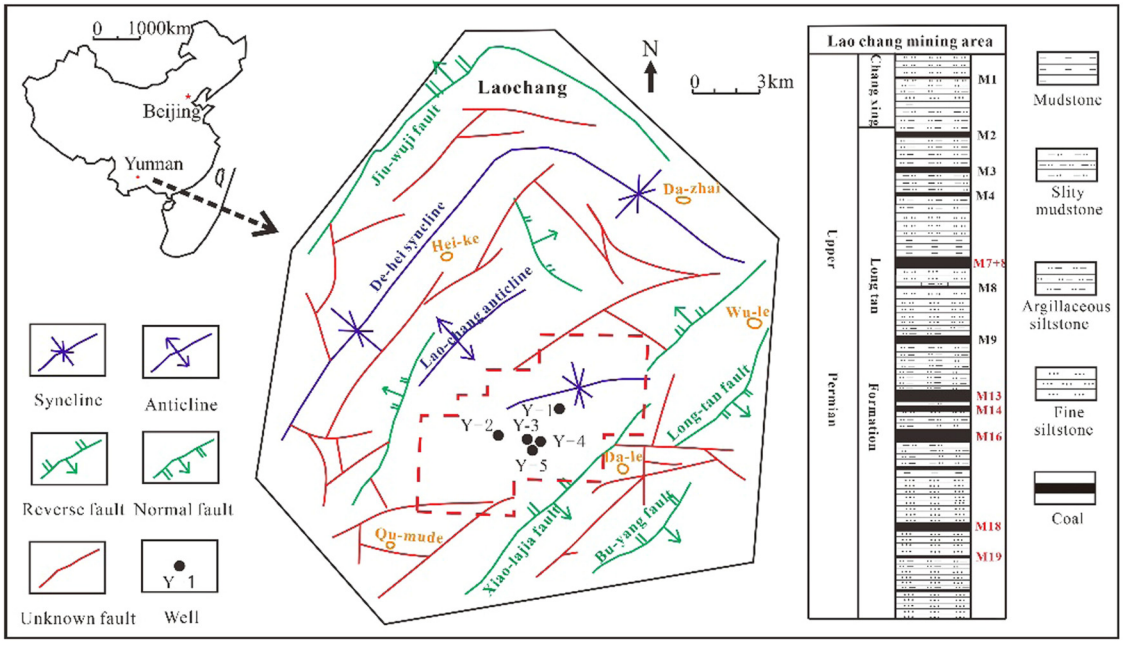

Figure 1: Study area structure and well location map.

Table 1: Characteristics of production wells

CBM wells	Water production date	Main coal seam	Depth (m)	Cumulative water production (m^3)	Cumulative gas production (m^3)
Y-1	Apr. 2018	7 + 8/13	717.9–780.0	297.17	27832.19
Y-2	Apr. 2018	16/18/19	698.5–735.6	395.60	35357.89
Y-3	May 2018	13/16/18/19	665.3–681.9	474.91	77461.46
Y-4	Jun. 2018	13/19	750.0–789.2	355.57	12341.49
Y-5	May 2018	14/16/18	687.4–745.8	398.76	72798.60

There are five CBM development test wells (Well Y-1, Y-2, Y-3, Y-4, and Y-5) that adopted the "segmented fracturing, combined layer drainage" developmental mode in the Laochang Block. The data of the cumulative water and gas production of the five wells by September 2018 are presented in Table 1. Well Y-3 produced most gas (77461.46 m^3) during this period, followed by wells Y-5, Y-2, Y-1, and Y-4. Well Y-3 had the highest cumulative water production, at 474.91 m^3, followed by wells Y-5, Y-2, Y-4, and Y-1.

2.2 Samples

Since April 2018, five CBM wells in the Laochang Block have been tracking and collecting water samples. The water sample was uniformly collected using a 2.5 L pure water bottle directly from the wellhead. The samples were sent to the Institute of Geochemistry, Guiyang Academy of Chinese Sciences within 72 h. The experiments conducted include the determination of the conventional anion and cation mass concentration of the produced water, the determination of stable hydrogen and oxygen isotopes, and the determination of trace element mass concentration. As of September 2018, well Y-1 had been collected six times, well Y-2 had been collected six times, well Y-3 had been collected five times, well Y-4 had been collected four times, and well Y-5 had been collected five times. These test results are the basis for this analysis (Tables 2 and 3).

3 Results and discussion

3.1 Characteristics of conventional ions and variation with time

The water produced from CBM wells has similar ion characteristics, that is, Na^+, K^+, and Cl^- concentrations are higher, while Ca^{2+}, Mg^{2+}, and SO_4^{2-} concentrations are lower. It is generally believed that Ca^{2+} and Mg^{2+} are more abundant in an open groundwater environment, while Na^+, Cl^-, and HCO_3^- are more abundant in a closed groundwater environment [14,33,34]. The water produced from the five CBM wells shows the same result, that is, Na^+, Cl^-, and HCO_3^- concentrations are higher, K^+, Ca^{2+}, Mg^{2+}, SO_4^{2-}, and F^- concentrations are lower, and the SO_4^{2-} concentration of the Y-3 well and Y-5 well is the lowest (Table 2).

With the increase in the drainage time, the type of water produced from the Y-1 and Y-2 wells changed from Na–Cl to Na–Cl–HCO_3. The type of water produced from Y-3, Y-4, and Y-5 wells changed from Na–Cl to Na–HCO_3. The concentrations of K^+, Na^+, Ca^{2+}, Mg^{2+}, and Cl^- in the five wells fluctuated and decreased with time (Figure 2). The K^+ concentration in the Y-2 well changed more with time, followed by the Y-1 well, and the changes in the Y-3, Y-4, and Y-5 wells were the smallest. The Na^+ concentration of the five wells does not vary significantly with time. The variation trend with time of the Ca^{2+}, Mg^{2+}, and Cl^- concentrations in the five wells is similar to that of K^+ concentration. The concentration of SO_4^{2-} in wells Y-1, Y-2, Y-3, and Y-5 showed a decreasing trend, while SO_4^{2-} concentration in the Y-1 and Y-2 wells varied greatly with time. SO_4^{2-} concentration in the Y-4 well increased initially and then decreased with time. The HCO_3^- and F^- concentrations in the five wells increased with time, among which the HCO_3^- concentration increased in a similar range. Meanwhile, the change in F^- concentration in the Y-1, Y-2, and Y-4 wells showed larger temporal variations, while the change in F^- concentration in the Y-3 and Y-5 wells depicted smaller temporal variations.

With the increase in drainage time, the fracturing fluid gradually discharges, which reduces the concentrations of Na^+, K^+, Cl^-, Ca^{2+}, and Mg^{2+}, indicating the weakening of the water–rock interaction. The concentrations of HCO_3^- and F^- increase with time, showing that the produced water is groundwater in a closed environment with a higher degree of retention. This indicated that the water produced from the five wells is

Table 2: Conventional ion date, hydrogen, and oxygen isotope date from water samples

CBM wells	Date	K^+ (mg/L)	Na^+ (mg/L)	Ca^{2+} (mg/L)	Mg^{2+} (mg/L)	Cl^- (mg/L)	SO_4^{2-} (mg/L)	HCO_3^- (mg/L)	F^- (mg/L)	$\delta^{18}O$ (‰ V-SMOW)	δD (‰ V-SMOW)	PH
Y-1	Apr.2018	391.24	2337.93	22.77	9.62	3693.08	40.27	756.37	1.02	−9.82	−58.54	8.2
	May.2018	388.14	2841.09	21.73	11.96	3566.23	22.89	899.61	0.80	−10.09	−72.55	7.3
	Jun.2018	448.06	2507.00	5.79	11.28	3622.01	19.57	1085.56	0.82	−10.5	−70.69	7.5
	Jul.2018	430.12	2393.63	19.22	9.48	3192.00	15.89	1483.55	0.86	−10.42	−68.35	8.3
	Aug.2018	271.02	2127.24	15.31	7.69	2841.46	17.33	1687.00	1.24	−10.71	−71.73	8.5
	Sep.2018	160.01	2006.09	12.35	5.08	2242.71	12.93	1830.97	1.24	−11.03	−72.2	8.4
	Mean	348.10	2368.83	16.19	9.18	3192.91	21.48	1290.51	1.00	−10.43	−69.01	8.0
Y-2	Apr.2018	653.81	3022.21	33.37	12.40	4742.68	34.82	1389.61	1.63	−10.47	−72.97	7.8
	May.2018	413.98	2979.60	22.48	8.59	3392.58	24.20	1683.62	1.52	−10.98	−82.04	7.2
	Jun.2018	360.69	2711.59	18.91	7.73	2941.82	24.38	1826.85	1.56	−11.68	−80.69	7.3
	Jul.2018	298.37	2416.54	16.39	6.57	2539.78	19.89	2400.60	1.55	−11.11	−76.28	8.0
	Aug.2018	233.85	2202.94	17.20	5.54	2112.89	17.87	2519.54	1.83	−11.76	−82.18	8.3
	Sep.2018	242.97	2191.07	12.93	4.85	2315.70	14.61	2463.20	2.11	−11.9	−83.77	8.2
	Mean	367.28	2587.32	20.21	7.61	3007.57	22.63	2047.24	1.70	−11.32	−79.65	7.8
Y-3	May.2018	362.71	3228.39	19.29	9.29	3436.52	0.37	2168.60	0.49	−11.59	−78.69	7.3
	Jun.2018	330.54	3123.74	14.79	8.89	3235.61	0.19	2291.73	0.60	−11.76	−79.1	7.7
	Jul.2018	276.25	2883.28	20.35	7.92	2813.12	0.20	2967.11	0.52	−11.09	−74.36	7.7
	Aug.2018	235.56	2734.76	22.92	7.11	2702.08	0.32	3045.35	0.54	−11.89	−78.54	7.9
	Sep.2018	206.35	2564.84	17.49	5.46	2454.66	0.46	3170.55	0.66	−11.69	−79.46	7.9
	Mean	282.28	2907.00	18.97	7.73	2928.40	0.31	2728.67	0.56	−11.6	−78.03	7.7
Y-4	Jun.2018	227.40	2270.35	10.42	5.70	2302.85	0.05	1756.49	1.38	−12.11	−82.41	8.1
	Jul.2018	174.65	2077.51	11.55	4.81	1995.86	3.88	2125.18	1.22	−11.37	−77.65	8.1
	Aug.2018	150.75	1867.78	15.81	4.42	1811.29	4.24	2225.33	1.71	−11.49	−81.43	8.4
	Sep.2018	136.65	1766.55	9.44	3.36	1554.92	3.33	2322.36	1.74	−12.03	−83.38	8.2
	Mean	172.36	1995.55	11.81	4.57	1916.23	2.87	2107.34	1.51	−11.75	−81.22	8.2
Y-5	May.2018	348.91	2609.78	9.92	7.31	2637.24	3.87	1884.65	0.60	−11.95	−82.34	7.6
	Jun.2018	299.72	2501.88	7.52	6.54	2525.99	1.61	1939.93	0.67	−11.92	−82.20	8.1
	Jul.2018	259.45	2316.31	11.08	6.55	2383.26	1.13	2381.82	0.55	−11.25	−77.20	8.1
	Aug.2018	213.25	2093.49	15.42	5.50	2171.06	0.29	2488.24	0.72	−12.12	−81.70	8.2
	Sep.2018	197.32	2006.94	11.07	4.38	1910.23	0.74	2600.91	0.70	−12.03	−83.96	8.1
	Mean	263.73	2305.68	11.00	6.06	2325.56	1.53	2259.11	0.65	−11.86	−81.48	8.0

characterized by closed groundwater, and the water–rock interaction of the Y-3 and Y-5 wells is more stable than that of the Y-1, Y-2, and Y-4 wells, as shown in Figure 2.

3.2 Characteristics of hydrogen and oxygen isotopes and variation with time

The hydrogen and oxygen isotope values of the water produced in the CBM wells are distributed near the atmospheric precipitation line. The hydrogen and oxygen isotope composition research method adopt the Yunnan atmospheric precipitation line equation: $\delta D = 6.56\ \delta^{18}O - 2.96$ [35].

Because the produced water is derived from the mixture of atmospheric precipitation, surface water, and groundwater, it generally exhibits significant D-drift characteristics or O-drift characteristics [24,36,37].

The water isotope values of the Y-1 and Y-3 wells are basically located to the left of the atmospheric precipitation line, showing D-drift characteristics (the Y-1 well exhibits O-drift characteristics on the right side of the atmospheric precipitation line in May), while the isotope values of the Y-2 and Y-4 wells are mostly located on the right side of the atmospheric precipitation line, showing O-drift characteristics. The isotope value of the water produced in the Y-5 well fluctuates on the atmospheric precipitation line and exhibits insignificant D-drift or O-drift characteristics (Figure 3).

In the reducing environment of coal measures, hydrogen and oxygen isotope drift in the formation water can be caused by isotope exchanges of minerals in the formation water rich in light isotopes such as H and ^{16}O; coal seams rich in heavy isotopes such as D and ^{18}O,

Table 3: Test data of trace elements in produced water

CBM wells	Date	Li (μg/L)	Ba (μg/L)	Sr (μg/L)	Rb (μg/L)	Mn (μg/L)	As (μg/L)
Y-1	Apr. 2018	636.40	786.40	6305.70	138.40	110.60	0.79
	May 2018	553.29	1085.81	15573.14	108.88	43.57	0.97
	Jun. 2018	607.41	1155.50	15150.34	122.26	136.16	0.49
	Jul. 2018	839.27	910.09	10398.55	133.99	134.01	0.74
	Aug. 2018	689.23	652.18	4618.43	101.28	150.97	0.50
	Sep. 2018	964.36	606.34	4322.43	85.82	162.35	1.03
	Mean	714.99	866.05	9394.76	115.11	122.94	0.75
Y-2	Apr. 2018	447.00	1718.90	8945.50	143.80	242.30	0.79
	May. 2018	328.44	1445.35	13106.44	95.87	135.98	0.90
	Jun. 2018	330.90	1229.76	10888.72	83.89	112.36	0.63
	Jul. 2018	491.07	1062.38	8081.89	87.67	135.67	0.77
	Aug. 2018	401.40	926.87	4035.61	75.89	89.81	0.96
	Sep. 2018	611.73	1042.32	4851.31	85.03	89.43	1.75
	Mean	435.09	1237.60	8318.25	95.36	134.26	0.97
Y-3	May 2018	585.42	6372.22	16419.17	100.29	151.96	0.73
	Jun. 2018	485.44	4325.69	10880.58	68.54	103.00	0.68
	Jul. 2018	779.40	4062.65	9504.99	71.57	214.87	0.94
	Aug. 2018	635.03	1698.04	4988.76	59.74	183.61	1.04
	Sep. 2018	964.92	2004.51	5542.35	62.54	197.87	2.78
	Mean	690.04	3692.62	9467.17	72.54	170.26	1.23
Y-4	Jun. 2018	459.37	1902.53	7734.81	48.22	56.06	0.39
	Jul. 2018	629.67	1663.16	6153.24	43.58	136.24	0.77
	Aug. 2018	483.35	1708.09	3101.90	36.30	94.26	0.71
	Sep. 2018	718.12	1786.39	3415.53	38.21	118.75	1.19
	Mean	572.63	1765.04	5101.37	41.58	101.33	0.76
Y-5	May 2018	644.30	1923.74	9617.75	75.44	56.30	0.32
	Jun. 2018	662.97	2169.40	7684.82	65.23	30.61	0.75
	Jul. 2018	1055.99	1915.36	7557.30	66.44	84.91	0.56
	Aug. 2018	852.83	2037.78	3922.86	53.44	61.44	0.63
	Sep. 2018	1284.98	1941.72	4206.15	54.44	85.69	1.18
	Mean	900.22	1997.60	6597.77	63.00	63.79	0.69

and the wall rock. In addition, microorganisms can produce HDS in a weakly alkaline and closed reduced coal seam environment. HDS dissolves in water and exchanges isotopes, which can also lead to the D-drift of formation water. Because of the enrichment of ^{18}O in carbonate strata, the oxygen-bearing mineral components in limestone are continuously dissolved in the process of runoff, which makes the heavier oxygen atoms in oxygen-bearing minerals easy to exchange with lighter oxygen atoms in limestone water, resulting in the continuous enrichment of ^{18}O in roof limestone water and ^{18}O isotope drift [25–28].

In the process of the fluid production, the following reactions may occur:

$$SO_4^{2-} + C(\text{organic}) + H_2O \rightarrow HDS + HCO_3^- \quad (1)$$

$$HDS + H_2O \rightarrow H_2S + HDS \quad (2)$$

$$H_2O \rightarrow H^+ + OH^- \quad (3)$$

$$H^+ + HCO_3^- \rightarrow H_2CO_3 \quad (4)$$

In the reduction environment of coal measures, sulfate can produce hydrogen sulfide, resulting in a decrease in SO_4^{2-} concentration, an increase in HCO_3^- concentration in the produced water, and the odor of hydrogen sulfide. It also reflects the fact that the produced water has the characteristics of coal seam water, equations (1) and (2). Because the produced water is weakly alkaline (Table 2), it can be inferred that there is a slight reaction of H^+ consumption (equations (3) and (4)).

The δD and $\delta^{18}O$ of the water produced in the Y-1 and Y-2 wells vary greatly with time, while those of the Y-3, Y-4, and Y-5 wells change slightly (Figure 4), indicating that the coal seams and surrounding rocks have great influence on the water produced in the Y-1 and Y-2 wells, but relatively small influence on the water produced in the Y-3, Y-4, and Y-5 wells. In August, δD and $\delta^{18}O$ of the five wells decreased with time, probably due to seasonal precipitation. Even in September, δD and $\delta^{18}O$ of the five wells decreased with time, but the

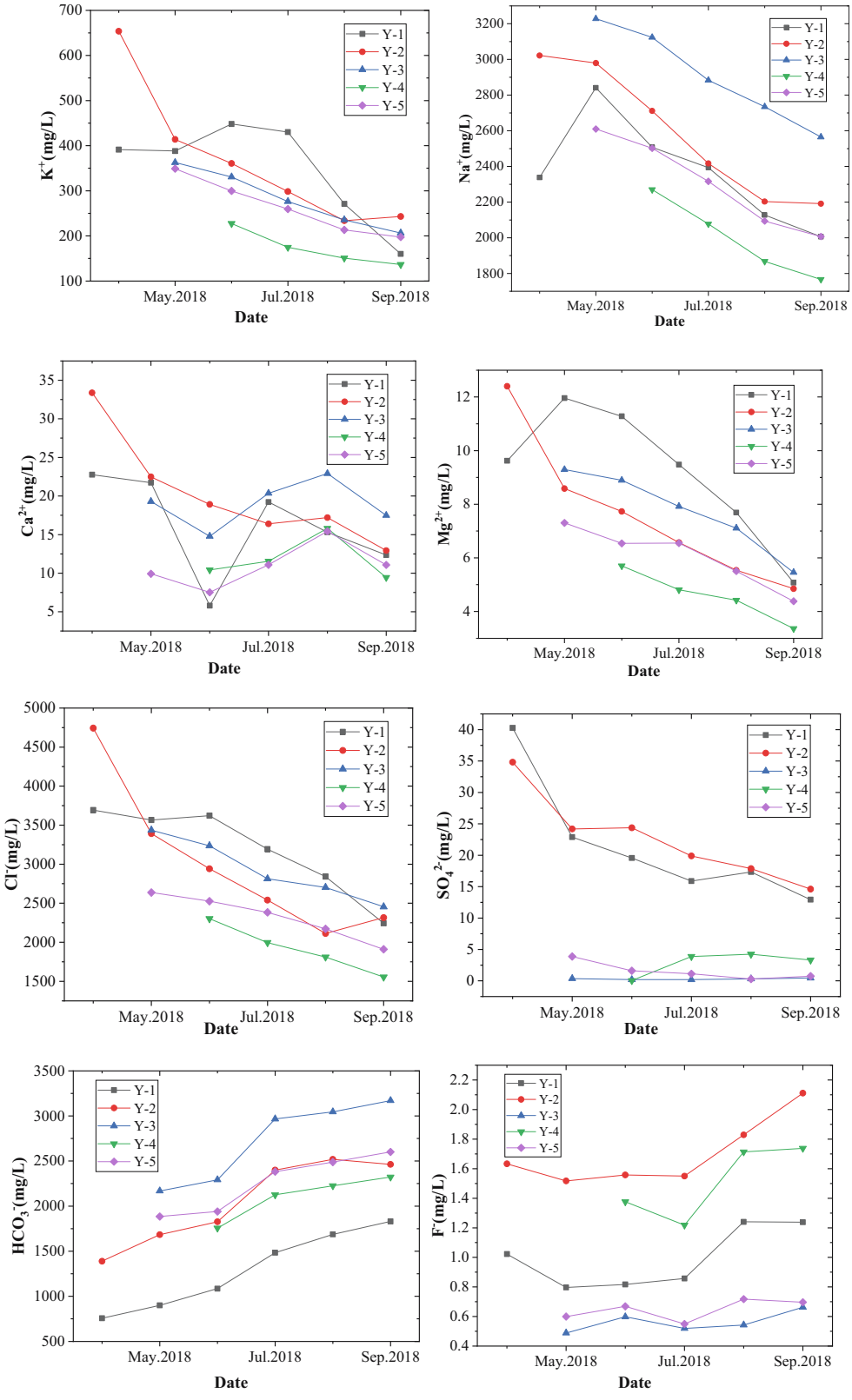

Figure 2: Ion concentration changes with time.

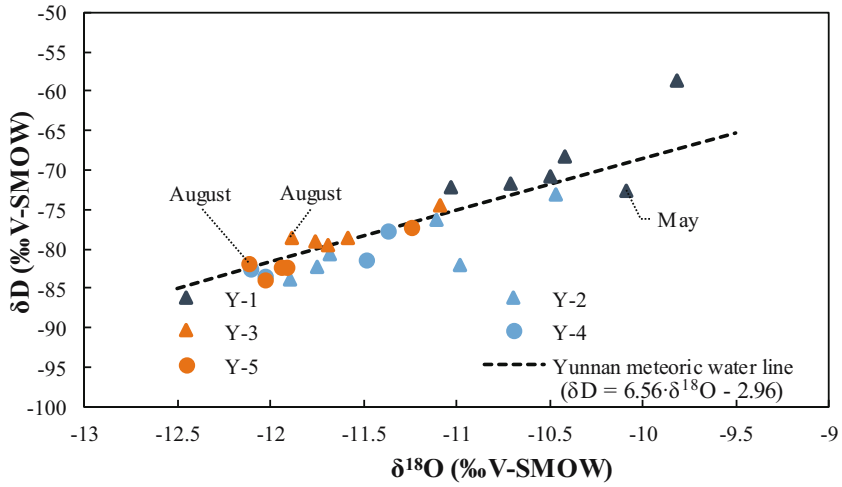

Figure 3: δD, $\delta^{18}O$ isotope relationship of the produced water.

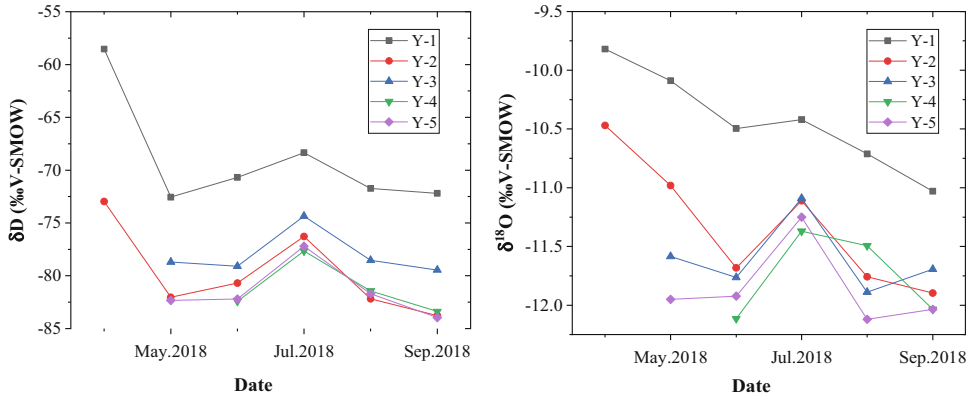

Figure 4: Temporal variations in δD, $\delta^{18}O$ isotopes in the produced water.

decline was less than that observed in August. The sudden increase in $\delta^{18}O$ of the Y-3 and Y-5 wells in September was probably due to the fluid penetration of the surrounding rock.

3.3 Characteristics of trace elements and variation with time

In the previous studies, the contents of Li, Ba, Sr, Rb, and Mn on the roof and floor are much higher than those in the coal seam, and their changes can indicate the change in the degree of influence of the roof and floor on the produced water. As, Hg, and Co mainly exist in the coal seam, and particularly, the high amounts of As in coal is a unique characteristic of this region [38–40].

With the increase in the drainage time, the trace elements Li, Mn, and As in the produced water of the five wells show an upward trend, while Ba, Sr, and Rb show a downward trend, and their changing trends are approximately the same (Figure 5). The reason may be that the water produced daily is gradually stabilized, and the water–rock reaction tends to be stable. Among them, the trace elements Ba and As in the Y-3 well vary greatly with time, which may be due to the continuous influence of the surrounding rock and coal seam on the produced water.

3.4 Effect of geochemical characteristics of produced water on gas well productivity

There has been considerable study on the impact on the production capacity of the production of water in the CBM wells [26,27]. Because Ca^{2+} and Mg^{2+} are the main elements of rock-forming minerals [41], and HCO_3^- and SO_4^{2-} mainly reflect the coal-bearing environment under

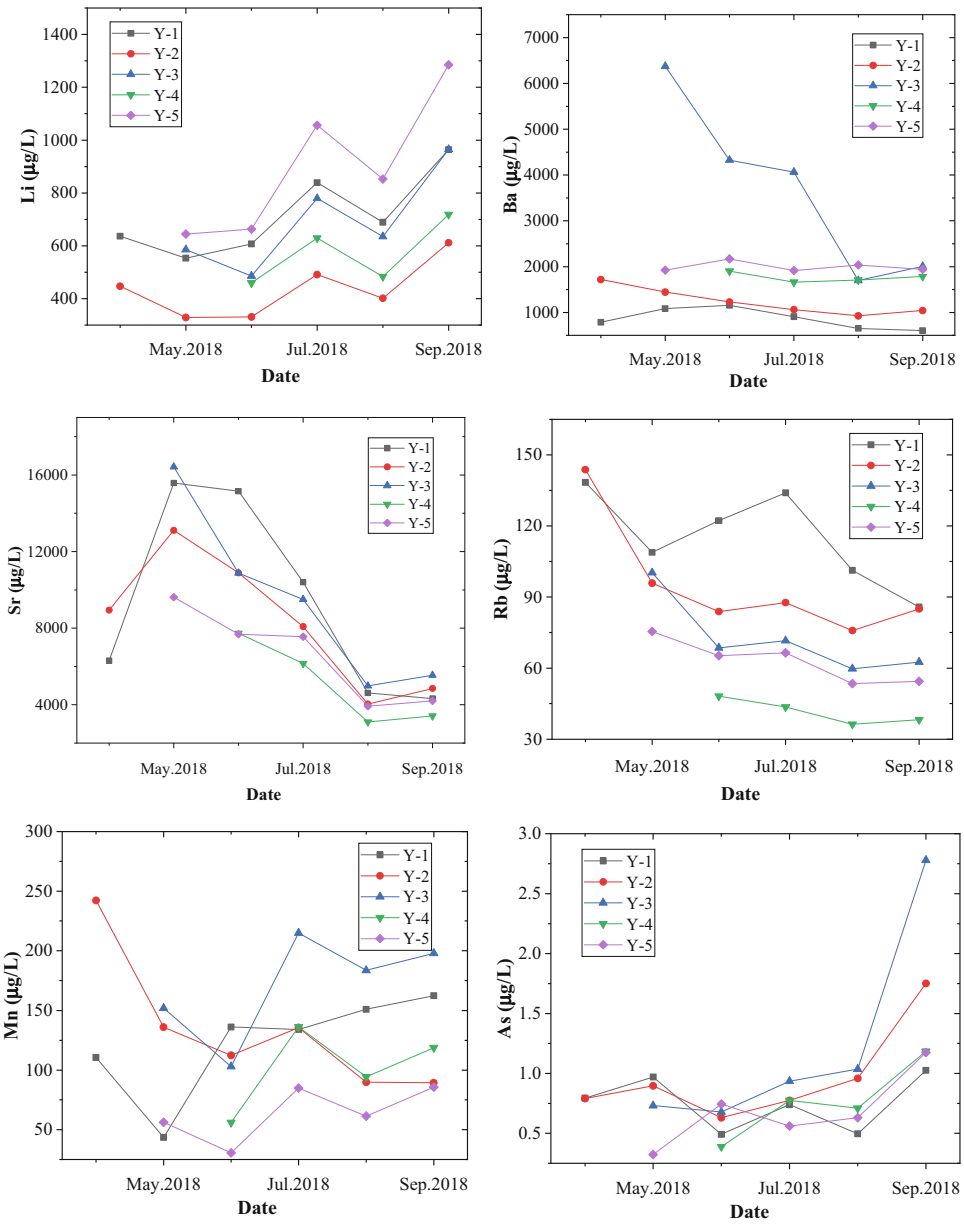

Figure 5: Changes of trace elements in the produced water with time.

closed conditions, based on previous studies and combined with the characteristics of the produced water and the changes in drainage and production curves in the study area, four characteristic ions – Ca^{2+}, Mg^{2+}, HCO_3^- and SO_4^{2-} – are selected to further analyze the relationship between the water production characteristics and productivity of the CBM wells. The degree of influence of the coal seam and surrounding rock on the produced water has dual effects on the gas production rate. Conversely, the degree of influence of the coal seam and surrounding rock on the produced water is greater, which can improve productivity. In addition, if it causes wellbore collapse or reservoir damage, it will be disadvantageous to productivity.

With the increase in the produced water in five CBM wells, δD and $\delta^{18}O$ show a downward trend in general, reflecting that the influence of coal seams and surrounding rocks on produced water is weakening, as shown in Figure 4. The reason may be the influence of the fracturing fluid on the produced water in the early stages of drainage. That is, with the gradual production of the fracturing fluid, the produced water gradually returns to the normal formation state, but in September, the $\delta^{18}O$ of the Y-3 and Y-5 wells suddenly increases.

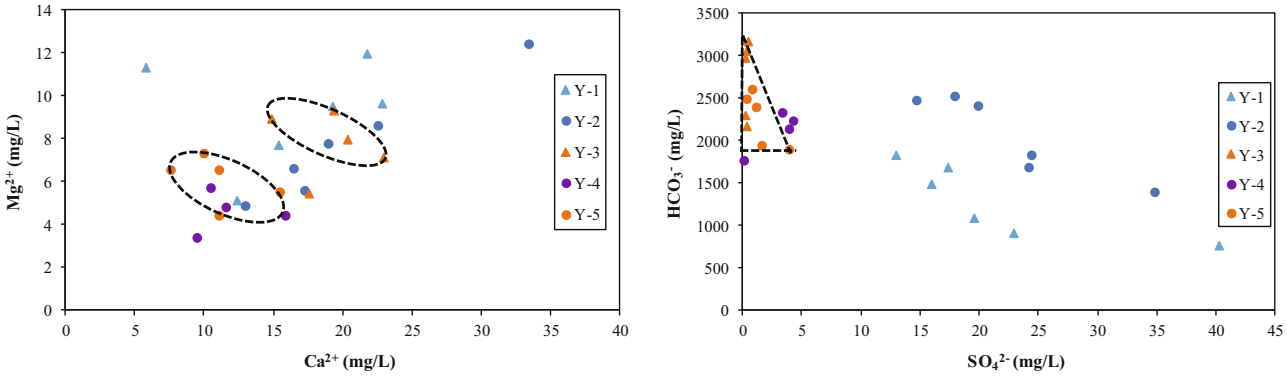

Figure 6: Distribution of characteristic ions in the produced water.

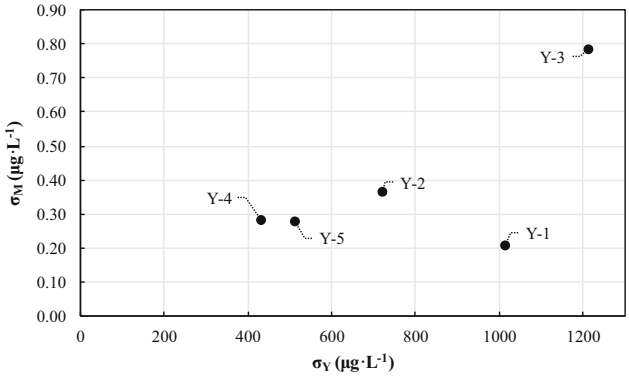

Figure 7: Standard deviation of trace elements in five wells in the study area (note: σ_Y denotes the discrete degree of the influence of the fracturing fluid on the surrounding rock; σ_M denotes the discrete degree of the influence of the fracturing fluid on the coal reservoir).

This suggests that the influence of the surrounding rock on the produced water is increasing because the surrounding rock is penetrated by the fluid.

According to the influence of trace elements on produced water, characteristic trace elements such as Li, Ba, Sr, Rb, Mn, and As were selected. By analyzing the standard deviation, the characterization parameters of the influence of the surrounding rock and coal seam on produced water were established.

$$\sigma_Y = \sigma(\text{Li}) + \sigma(\text{Ba}) + \sigma(\text{Sr}) + \sigma(\text{Rb}) + \sigma(\text{Mn}) \quad (5)$$

$$\sigma_M = \sigma(\text{As}) \quad (6)$$

Equation (5) denotes the discrete degree of the influence of the fracturing fluid on the surrounding rock, and the magnitude of the value indicates the fluctuation of the influence of the fracturing fluid on the surrounding rock, which can indirectly reflect the patency of the fluid passage. Equation (6) denotes the discrete degree of the influence of the fracturing fluid on the coal reservoir, and the magnitude of the value can indirectly reflect the extent of the fracturing fluid expansion in the reservoir.

The standard deviations σ_Y and σ_M can indirectly reflect the extent of the influence of the fracturing fluid

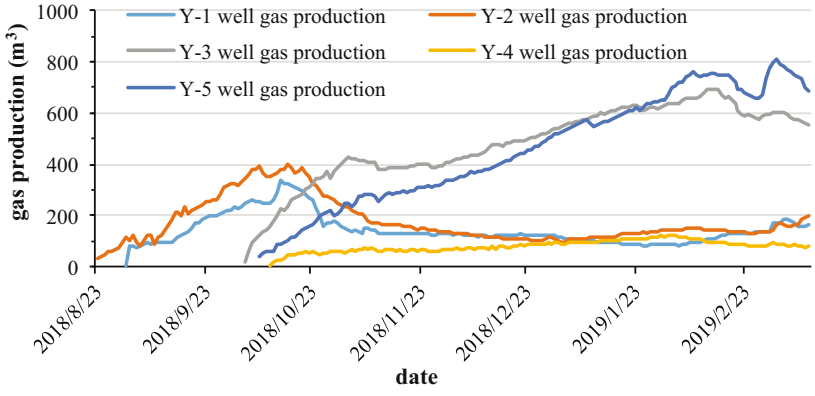

Figure 8: Gas production variation charts of five wells in the study area.

on the reservoir and surrounding rock. When σ_Y is large, wellbore collapse can easily occur, which is not conducive to the production of fluids. When σ_M is large, damage to the coal reservoir can easily occur, which is unfavorable to later gas production.

The Y-3 and Y-5 wells have the best production status, as shown in Figures 4–8. Moreover, it also reflects that the process that takes place in the Y-3 and Y-5 wells (ellipse and triangular areas in Figure 6) in the flow through the surrounding rocks, and coal seams is beneficial for enhancing productivity. However, the water produced in the Y-1, Y-2, and Y-4 wells in the process of flowing through surrounding rock and coal seam is not conducive to enhance productivity, which may be caused by wellbore collapse or reservoir damage [42,43]. Based on the characteristics of water produced in Y-3 and Y-5 wells with better drainage effect, the quantitative characterization range of produced water in high-production CBM wells is proposed: (1) δD is in the range of −85‰ to −75‰ with the fluctuation range spanning 5‰, $\delta^{18}O$ is in the range of −12‰ to −11‰ with the fluctuation range spanning 0.5‰, and the fluctuation range of Ca^{2+} spans 10 mg/L. The fluctuation range of Mg^{2+} spans 4 mg/L, the fluctuation range of SO_4^{2-} spans 3 mg/L, and the fluctuation range of HCO_3^- spans 1,000 mg/L. (2) $0 \le \sigma_M < 0.3$ and $0 \le \sigma_Y < 600$ (the influence of the surrounding rock and coal seam on produced water is relatively stable, taking the Y-5 well as an example, and the poor drainage effect of the Y-4 well is likely to be caused by human factors) or $0.7 < \sigma_M < 0.8$ and $1{,}200 < \sigma_Y < 1{,}300$ (the influence of the surrounding rock and coal seam on produced water fluctuates greatly, taking the Y-3 well as an example). Because the tracking time is not long and the number of CBM wells is limited, the characterization method proposed earlier will be further improved by more drainage data from the drainage wells.

4 Conclusions

In this article, the geochemical characteristics of conventional ions, trace elements, and hydrogen and oxygen isotopes in the produced water from five CBM wells in Laochang Block, Eastern Yunnan, and their relationship with productivity were analyzed, and the following conclusions were presented:

With the increase in the drainage time, the type of water produced in the Y-1 and Y-2 wells changed from Na-Cl to Na-Cl-HCO_3. The types of water produced in the Y-3, Y-4, and Y-5 wells also changed from Na-Cl to Na-HCO_3.

The concentrations of K^+, Na^+, Ca^{2+}, Mg^{2+}, and Cl^- in the five wells fluctuated and decreased with time. The concentration of SO_4^{2-} in Y-1, Y-2, Y-3, and Y-5 wells showed a decreasing trend with time. The HCO_3^- and F^- concentrations of the five wells showed a tendency to increase with time. The water produced in the five wells was characterized by closed groundwater, while the water–rock interactions in the Y-3 and Y-5 wells were more stable than those in the Y-1, Y-2, and Y-4 wells.

Four kinds of chemical reactions in different stages of the production process were proposed. With the increase in the produced water in the five CBM wells, δD and $\delta^{18}O$ show a downward trend in general, suggesting that the influence of coal seams and surrounding rocks on the produced water is weak. In September, $\delta^{18}O$ of the Y-3 and Y-5 wells suddenly increases, indicating that the influence of the surrounding rock on the produced water is increasing, because the surrounding rock is penetrated by fluid. Combining with the water production characteristics of the Y-3 and Y-5 wells with better drainage and recovery effects, it is proposed that $0 \le \sigma_M < 0.3$ and $0 \le \sigma_Y < 600$ or $0.7 < \sigma_M < 0.8$ and $1{,}200 < \sigma_Y < 1{,}300$, and the fluctuation ranges of Ca^{2+}, Mg^{2+}, HCO_3^-, and SO_4^{2-} can be used to quantitatively characterize and evaluate the productivity of the CBM wells.

Funding: This research was funded by the National Natural Science Foundation of China (no. 41572140 and 41872170), the National Major Special Project of Science and Technology of China (no. 2016ZX05044), the National Natural Science Foundation Project (no. 41802181), the Natural Science Foundation Project of Jiangsu Province (no. BK20180660), and the Qing Lan Project.

Conflict of interest: The authors declare no conflict of interest.

References

[1] Ye J, Wu Q, Wang Z. Controlled characteristics of hydrogeological conditions on the coalbed methane migration and accumulation. J China Coal Soc. 2001;26:459–62.

[2] Guo C, Xia Y, Ma D, Sun X, Dai G, Shen J, et al. Geological conditions of coalbed methane accumulation in the Hancheng area, southeastern Ordos Basin, China: implications for coalbed methane high-yield potential. Energy Explor Exploit. 37;2019:922–44.

[3] Tao S, Chen S, Tang D, Zhao X, Xu H, Li S. Material composition, pore structure and adsorption capacity of low-rank coals around the first coalification jump: a case of eastern Junggar Basin, China. Fuel. 2018;211:804–15.
[4] Bachu S, Michael K. Possible controls of hydrogeological and stress regimes on the producibility of coalbed methane in upper Cretaceous-Tertiary strata of the Alberta Basin, Canada. AAPG Bull. 2003;87:1729–54.
[5] Colmenares L, Zoback M. Hydraulic fracturing and wellbore completion of coalbed methane wells in the Powder River Basin, Wyoming: implications for water and gas production. AAPG Bull. 2007;91:51–67.
[6] Pashin J, McIntyre-Redden M, Mann S, Kopaska-Merkel D, Varonka M, Orem W. Relationships between water and gas chemistry in mature coalbed methane reservoirs of the Black Warrior Basin. Int J Coal Geol. 2014;126:92–105.
[7] Zhang J, Liu D, Cai Y, Pan Z, Yao Y, Wang Y. Geological and hydrological controls on the accumulation of coalbed methane within the No. 3 coal seam of the southern Qinshui Basin. Int J Coal Geol. 2017;182:94–111.
[8] Zhang X, Wu C, Liu S. Characteristic analysis and fractal model of the gas-water relative permeability of coal under different confining pressures. J Pet Sci Eng. 2017;159:488–96.
[9] Liu X, Wu C. Simulation of dynamic changes of methane state based on NMR during coalbed methane output. Fuel. 2017;194:188–94.
[10] Tao S, Pan Z, Tang S, Chen S. Current status and geological conditions for the applicability of CBM drilling technologies in China: a review. Int J Coal Geol. 2019;202:95–108.
[11] Karacan C, Goodman G. Analyses of geological and hydrodynamic controls on methane emissions experienced in a Lower Kittanning coal mine. Int J Coal Geol. 2012;98:110–27.
[12] Moore T. Coalbed methane: a review. Int J Coal Geol. 2012;101:36–81.
[13] Qin S, Tang X, Song Y, Wang H. Distribution and fractionation mechanism of stable carbon isotope of coalbed methane. Sci China Ser D Earth Sci. 2006;49:1252–8.
[14] Van Voast W. Geochemical signature of formation waters associated with coalbed methane. AAPG Bull. 2003;87:667–76.
[15] Wang B, Sun F, Tang D, Zhao Y, Song Z, Tao Y. Hydrological control rule on coalbed methane enrichment and high yield in FZ Block of Qinshui Basin. Fuel. 2015;140:568–77.
[16] Tao S, Pan Z, Chen S, Tang S. Coal seam porosity and fracture heterogeneity of marcolithotypes in the Fanzhuang Block, southern Qinshui Basin, China. J Na Gas Sci Eng. 2019;66:148–58.
[17] Mitcham S, Wobeser G. Effects of sodium and magnesium sulfate in drinking water on mallard ducklings. J Wildl Dis. 1988;24:30–44.
[18] Singh A, Gupta S, Mendhe V, Mishra S. Variations in hydrochemical properties and source insights of coalbed methane produced water of Raniganj Coalfield, Jharkhand, India. J Na Gas Sci Eng. 2018;51:233–50.
[19] Wu C, Yao S, Du Y. Production systems optimization of a CBM well based on a time series BP neural network. J China Univ Min Technol. 2015;44:64–69.
[20] Frape S, Fritz P, McNutt R. Water-rock interaction and chemistry of groundwater from the Canadian Shield. Geochim Cosmochim Acta. 1984;48:1617–27.
[21] Alley B, Beebe A, Rodgers J, Castle J. Chemical and physical characterization of produced waters from conventional and unconventional fossil fuel resources. Chemosphere. 2011;85:74–82.
[22] Zhou B, Qin Y, Yang Z. Ion composition of produced water from coalbed methane wells in western Guizhou, China, and associated productivity response. Fuel. 2020;265:116939.
[23] Sowder J, Kelleners T, Reddy K. The origin and fate of arsenic in coalbed natural gas-produced water ponds. J Environ Qual. 2010;39:1604–15.
[24] Abu B, Zarrouk S. Geochemical multiaquifer assessment of the Huntly coalfield, New Zealand, using a novel chloride-bicarbonate-boron ternary diagram. Int J Coal Geol. 2016;167:136–47.
[25] Wei M, Ju Y. Chemical characteristics and origin of produced waters from coalbed gas field in the southern of Qinshui Basin. J China Coal Soc. 2015;40:629–35.
[26] Wu C, Yang Z, Qin Y, Chen J, Zhang Z, Li Y. Characteristics of hydrogen and oxygen isotopes in produced water and productivity response of coalbed methane wells in Western Guizhou. Energy Fuels. 2018;32:11203–11.
[27] Guo C, Qin Y, Xia Y, Ma D, Han D. Source discrimination of produced water from CBM commingling wells based on the hydrogen and oxygen isotopes: a case study of the Upper Permian, Bide-Santang Basin,western Guizhou area. Acta Petrol Sin. 2017;38:493–501.
[28] Li W, Qin S. Characteristics of trace elements and hydrogen and oxygen isotopes in the formation water of the Xujiahe Formation, Sichuan Basin. Acta Petrol Sin. 2012;33:55–63.
[29] Qin Y, Zhang Z, Bai J, Liu D, Tian Y. Source apportionment of produced-water and feasibility discrimination of commingling CBM production from wells in Southern Qinshui Basin. J China Coal Soc. 2014;39:1892–98.
[30] Xu Z, Liu Q, Zheng Q, Cheng H, Wu Y. Isotopic composition and content of coalbed methane production gases and waters in karstic collapse column area, Qinshui Coalfield, China. J Geochem Explor. 2016;165:94–101.
[31] Zhu Y, Sun B, Zeng F, Xia P, Zhang P, You Y. Hydrogeological characteristics of CBM reservoirs and their controlling effects in Gujiao Mining Area, Xishan Coalfield. J China Coal Soc. 2018;43:759–69.
[32] Dahm K, Guerra K, Xu P, Drewes J. Composite geochemical database for coalbed methane produced water quality in the Rocky Mountain Region. Environ Sci Technol. 2011;45:7655–63.
[33] Taulis M, Milke M. Chemical variability of groundwater samples collected from a coal seam gas exploration well, Maramarua, New Zealand. Water Res. 2013;47:1021–34.
[34] Yang Z, Wu C, Zhang Z, Jin J, Zhao L, Li Y. Geochemical significance of CBM produced water: a case study of developed test wells in Songhe block of Guizhou province. J China Univ Min Technol. 2017;46:710–7.
[35] Hu H, Wang J. On Characteristics of Hydrogen and Oxygen Isotope in Precipitation in Yunnan and Analysis of Moisture Sources. J Southwest China Normal Univ (Nat Sci Ed). 2015;40:142–9.

[36] Dansgaard W. Stable isotopes in precipitation. Tellus. 1964;16:436–68.
[37] Mao Q, Wang J, Wang J, Li W. Analysis of the characteristics of δD and $\delta^{18}O$ in the meteoric precipitation in Anshun, Guizhou province and Beibei Chongqing. J Southwest Univ (Nat Sci Ed). 2017;39:114–20.
[38] Chen P, Kuang H, Tang X. Research on the distribution and occurrence of arsenic in coal. J China Coal Soc. 2002;27:259–63.
[39] Li D, Chen K, Deng T, Cheng F, Yang J. Distribution and enrichment factors of arsenic in coals of Southwestern China. J China Univ Min Technol. 2002;31:419–22.
[40] Wang M, Zheng B, Hu J, Li S, Wang B. Distribution of arsenic in southwest coals. J China Coal Soc. 2005;30:344–8.
[41] Guo C, Qin Y, Han D. Ions dynamics of produced water and indication for CBM production from wells in Bide-Santang Basin, Western Guizhou. J China Coal Soc. 2017;42: 680–6.
[42] Zhang X, Wu C, Liu Q. Study on drainage system of coalbed methane well based on drainage rate. Coal Sci Technol. 2015;43:131–5.
[43] Yang Z, Qin Y, Wu C, Qin Z, Li G, Li C. Geochemical response of produced water in the CBM well group with multiple coal seams and its geological significance – a case study of the Songhe well group in Western Guizhou. Int J Coal Geol. 2019;207:39–51.